ChemPubSoc Europe

DOI: 10.1002/chem.201600853

CHEMISTRY
A European Journal
Communication

Nanozymes

Chiral Nanozymes–Gold Nanoparticle-Based Transphosphorylation Catalysts Capable of Enantiomeric Discrimination

Jack L.-Y. Chen, Cristian Pezzato, Paolo Scrimin, and Leonard J. Prins*[a]

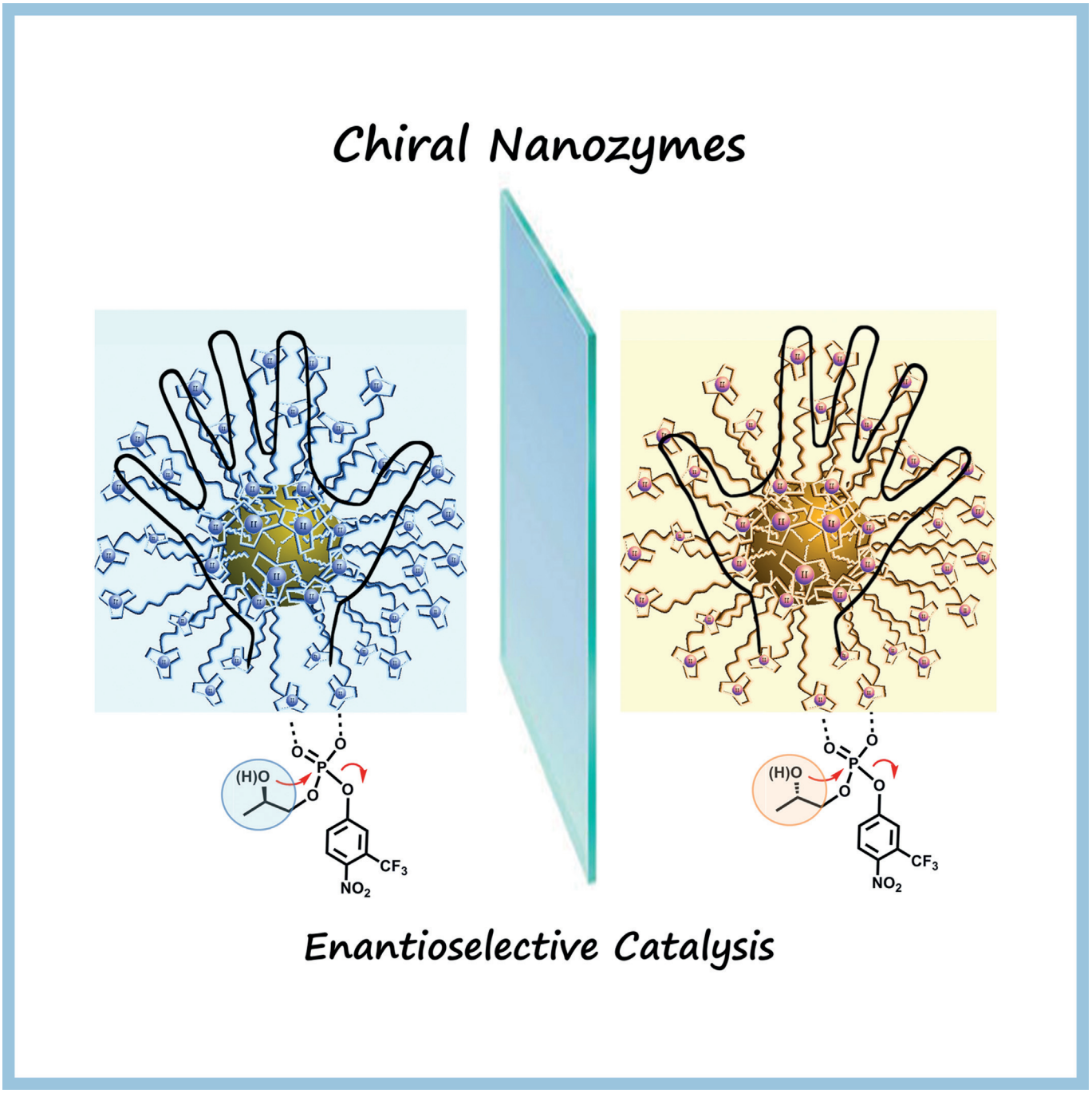

Abstract: Enantioselectivity in RNA cleavage by a synthetic metalloenzyme has been demonstrated for the first time. Thiols containing chiral Zn^{II}-binding head groups have been self-assembled on the surface of gold nanoparticles. This results in the spontaneous formation of chiral bimetallic catalytic sites that display different activities (k_{cat}) towards the enantiomers of an RNA model substrate. Substrate selectivity is observed when the nanozyme is applied to the cleavage of the dinucleotides UpU, GpG, ApA, and CpC, and remarkable differences in reactivity are observed for the cleavage of the enantiomerically pure dinucleotide UpU.

Chemists have long been fascinated with the complexity and efficiency of Nature's enzymes. This has led to the development of numerous synthetic systems that try to emulate the properties of this natural machinery.[1] Recently, gold nanoparticles (AuNPs) passivated by thiols which terminate with metal complexes[2] have been shown to possess many features of metalloenzymes.[3] These include the cooperativity between neighboring metal ions and Michaelis–Menten kinetics in the cleavage of phosphodiester bonds.[2b] These AuNPs have thus emerged as an attractive platform for the development of synthetic enzymes[4] and, in particular, as a model[5] for nucleases. However, despite the large body of work dedicated to synthetic metalloenzymes for RNA cleavage,[2,5,6] there are to the best of our knowledge no studies aimed at enantiodifferentiation. This is a remarkable fact considering that enantioselectivity is one of the hallmarks of enzyme catalysis.

Our aim was to employ AuNPs as a platform on which to self-assemble chiral precursors and generate an active catalyst capable of enantiodiscrimination. This goal is fundamentally different to the immobilization of known and established chiral catalysts onto gold nanoparticles (or other solid supports).[7] In our proposed system, the individual thiols only represent half the catalytic site, and its self-assembly on the surface of the gold nanoparticle is essential for formation of the active catalyst. In fact, it has been shown previously that the individual metal complexes are poorly active for the transphosphorylation of a RNA model substrate when free in solution,[2c] giving further importance to the self-assembly process. Herein, we report that chiral metal-binding thiols are indeed able to self-assemble on the surface of AuNPs to form active catalysts and exhibit different reactivity for the enantiomers of a pure RNA model substrate. Subsequently, by taking advantage of the multivalent nature of the nanozyme, additional binding interactions with dinucleotides were exploited to induce substrate selectivity in the cleavage of UpU, GpG, ApA, and CpC and enantioselectivity in the cleavage of UpU. The ability to display enantioselective catalysis brings these synthetic nanosystems another step closer to mimicking enzymes.

We have prepared two batches of NPs (Figure 1), each coated with a self-assembled monolayer of enantiomerically pure thiols where the chirality of the head group is derived from either L or D serine.[8] To ensure nanoparticle uniformity,

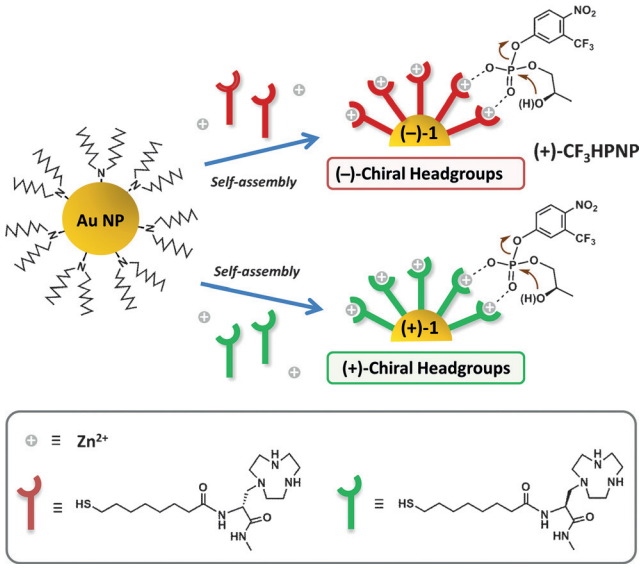

Figure 1. Schematic representation of the self-assembly of thiols containing chiral head groups on the surface of dioctylamine-passivated gold nanoparticles to form **(+)-1** and **(–)-1** NPs, which are active for the catalysis of CF_3HPNP. CF_3HPNP = 2-hydroxypropyl *p*-nitro-*m*-trifluoromethylphenyl phosphate. Only one hemisphere of the **(+)-1** and **(–)-1** NPs is shown.

the two batches of NPs **(+)-1** and **(–)-1** were synthesized from a single batch of dioctylamine-coated NPs prepared using a modified version of the procedure by Peng et al.[9] This involved initial stabilization of the gold nanoparticles by a weakly coordinating ligand, which allowed for uniform size distribution, prior to final stabilization by the addition of thiols. The resulting well-distributed sub-2 nm gold NPs were split into two, before introduction of the corresponding enantiomeric thiols to each batch. The final NPs **(+)-1** and **(–)-1** were analyzed by ^{1}H NMR, UV spectroscopy, transmission electron microscopy (TEM), and dynamic light scattering (DLS) and found to be identical (see the Supporting Information). Thermogravimetric analysis also confirmed that the loading of thiols onto **(+)-1** and **(–)-1** NPs were the same. Critically, circular dichroism (CD) measurements displayed equal and opposite signals at 204 nm for NPs **(+)-1** and **(–)-1**, reflecting the presence of thiols of opposite chirality on the NP surface.

The thiols employed in the above-mentioned self-assembly terminate with triazacyclononane (TACN) metal-binding units. The resulting complexes with Zn^{II} are the crucial elements for cleaving the phosphodiester moiety of an RNase substrate. Previous studies have shown that at least two neighboring metal ions work cooperatively (see Figure 1).[5f] At this point, we needed to synthesize enantiomerically pure RNA model

[a] *Dr. J. L.-Y. Chen, Dr. C. Pezzato, Prof. Dr. P. Scrimin, Prof. Dr. L. J. Prins*
Department of Chemical Sciences, University of Padova
Via Marzolo 1, 35131 Padova (Italy)
E-mail: leonard.prins@unipd.it

Supporting information for this article and ORCID for the corresponding author are available on the WWW under http://dx.doi.org/10.1002/chem.201600853.

substrates to verify whether the NPs **(+)-1** and **(−)-1** were capable of enantioselective catalysis.

We chose to pursue the synthesis of 2-hydroxypropyl *p*-nitro-*m*-trifluoromethylphenyl phosphate **(+)-2** (CF_3HPNP; Scheme 1), a trifluoromethyl-substituted analogue of 2-hydroxypropyl *p*-nitrophenyl phosphate (HPNP). This more reactive substrate gave greater flexibility when probing different reaction conditions (such as changes in pH) to gauge any differences in the catalytic activity of the NPs **(+)-1** and **(−)-1**. The required chiral substrate was synthesized beginning with the condensation of 3-trifluoromethyl-4-nitrophenol and phosphorus oxychloride (Scheme 1),[10] followed by further condensation with chiral alcohol **3**,[6d] which provided the optically pure chiral center. Desilylation of the resulting triethylamine salt and cation exchange then provided the desired optically pure (+)-CF_3HPNP **(+)-2** as a Na^+ salt. This same procedure

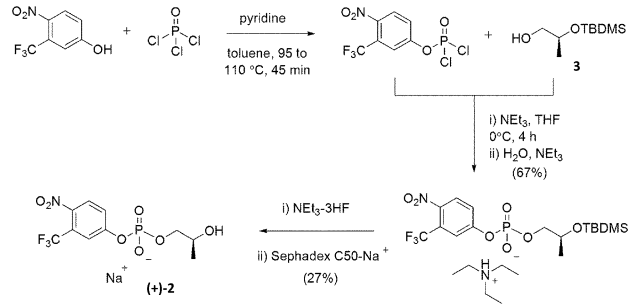

Scheme 1. Synthesis of chiral substrate (+)-CF_3HPNP.[6d,10]

was followed using the opposite enantiomer of alcohol **3** for the synthesis of the enantiomeric (−)-CF_3HPNP, **(−)-2**.

Initial studies in aqueous buffer, using the nanoparticle catalysts ([TACN·Zn^{II}] = 5 μM) and the (+)-CF_3HPNP substrate (2 μM) immediately garnered interesting results. A plot of the absorbance at 405 nm, corresponding to the presence of product, revealed a clear difference in the hydrolysis rate of (+)-CF_3HPNP in the presence of either **(+)-1** or **(−)-1** NPs (Figure 2a). Fitting of the curves to pseudo-first-order kinetics revealed the k_{obs} value for the hydrolysis in the presence of **(−)-1** NP to be $1.1 \pm 0.1 \times 10^{-4}$ s^{-1}, almost half the k_{obs} in the presence of **(+)-1** NP ($2.0 \pm 0.1 \times 10^{-4}$ s^{-1}). Control experiments using the enantiomeric (−)-CF_3HPNP with NPs **(+)-1** and **(−)-1**, revealed an inversion in the curves obtained from the above experiment, with a k_{obs} of $2.1 \pm 0.1 \times 10^{-4}$ s^{-1} observed with **(−)-1** NP and $1.1 \pm 0.1 \times 10^{-4}$ s^{-1} observed with **(+)-1** NPs. This important control using the opposite enantiomer of the original substrate left no doubt that the observed difference in reaction rate was indeed due to a difference in the chiral environment on the surface of the gold nanoparticles.

A surprising insight into the origin of this difference was obtained from a study of the catalytic activity of **(+)-1** and **(−)-1** NPs at varying concentrations of the (+)-CF_3HPNP substrate ([TACN·Zn^{II}] = 10 μM, pH 6.5). A plot of the initial reaction rates with respect to (+)-CF_3HPNP concentration revealed significantly different profiles between **(+)-1** and **(−)-1** NPs (Figure 2b). Fitting of the saturation profiles to the Michaelis–Menten equation yielded a k_{cat} value of $2.5 \pm 0.1 \times 10^{-3}$ s^{-1} for **(−)-1** NPs, whereas for **(+)-1** NPs a 38% higher value was ob-

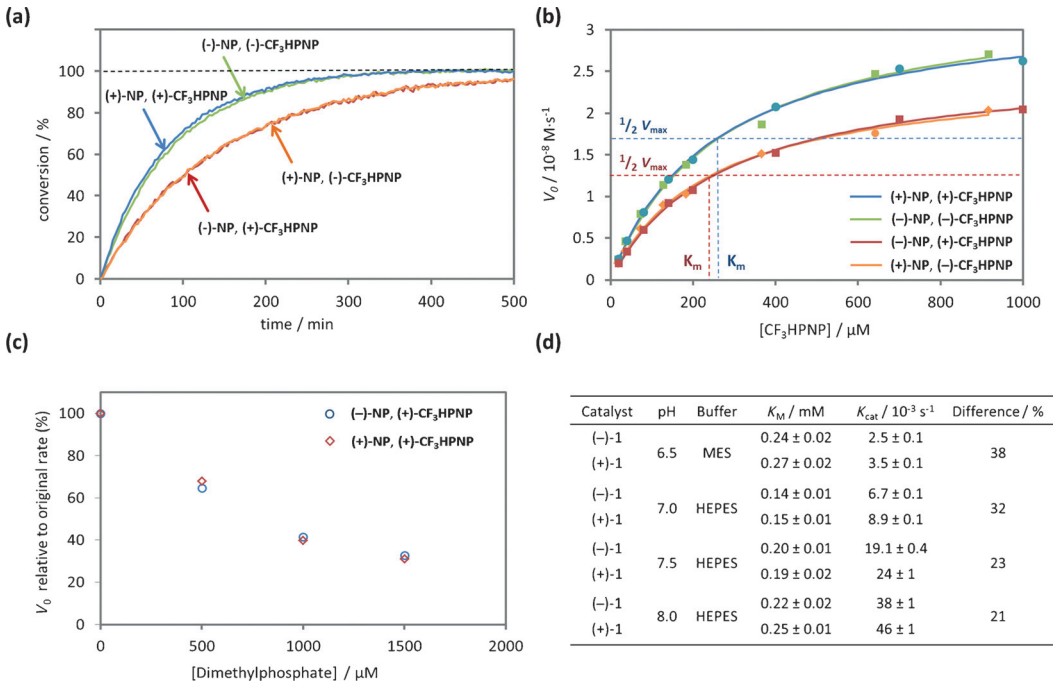

Catalyst	pH	Buffer	K_M / mM	K_{cat} / 10^{-3} s^{-1}	Difference / %
(−)-1	6.5	MES	0.24 ± 0.02	2.5 ± 0.1	38
(+)-1			0.27 ± 0.02	3.5 ± 0.1	
(−)-1	7.0	HEPES	0.14 ± 0.01	6.7 ± 0.1	32
(+)-1			0.15 ± 0.01	8.9 ± 0.1	
(−)-1	7.5	HEPES	0.20 ± 0.01	19.1 ± 0.4	23
(+)-1			0.19 ± 0.02	24 ± 1	
(−)-1	8.0	HEPES	0.22 ± 0.02	38 ± 1	21
(+)-1			0.25 ± 0.01	46 ± 1	

Figure 2. a) Catalysis of (+)- or (−)-CF_3HPNP (2 μM) by **(+)-1** or **(−)-1** NPs ([TACN] = 5 μM), as a percentage of conversion over time; HEPES pH 7.0 buffer (10 mM), $Zn(NO_3)_2$ (5 μM), 40 °C. b) Plot of initial reaction rates versus [CF3HPNP], showing fit with Michaelis–Menten kinetics; MES pH 6.5 buffer (10 mM), **(+)-1** or **(−)-1** NPs (10 μM), $Zn(NO_3)_2$ (10 μM), (+)- or (−)-CF_3HPNP (variable), 40 °C. c) Inhibition studies using dimethyl phosphate as inhibitor; MES pH 6.5 buffer (10 mM), **(+)-1** or **(−)-1** NPs (10 μM), $Zn(NO_3)_2$ (10 μM), dimethylphosphate (variable), 40 °C. d) Summary of Michaelis–Menten data at different pH values. See Supporting Information for further details.

tained ($k_{cat} = 3.5 \pm 0.1 \times 10^{-3}\ s^{-1}$). On the contrary, similar K_M (which is as a measure of binding affinity) values of 0.24 ± 0.02 mM and 0.27 ± 0.02 mM were obtained for **(−)-1** and **(+)-1** NPs, respectively. This is remarkable, considering that a different affinity of the chiral substrate for the enantiomeric NPs would be the most obvious explanation for the observed difference. However, considering that the K_M values are unchanged—this is clearly not the case. This was further confirmed by an inhibition experiment in which the catalytic activity was measured using substrate (+)-CF_3HPNP in the presence of increasing amounts of an achiral inhibitor—dimethylphosphate (Figure 2c). It can be seen that the extent of inhibition is the same for both **(+)-1** and **(−)-1** NPs, which confirms that (+)-CF_3HPNP has the same affinity for both NPs. Remarkably, the difference in catalytic activity originates from the difference in k_{cat} between **(+)-1** and **(−)-1** NPs (38% difference at pH 6.5). In enzymatic catalysis, k_{cat} is a first-order rate constant that refers to the efficiency of the enzyme in catalyzing the chemical transformation and is often referred to as the turnover number. This implies that the difference in catalytic activity can be attributed to energy differences in the respective transition states that are formed when (+)-CF_3HPNP reacts on the surface of **(+)-** and **(−)-1** NPs. This is an exciting observation as it demonstrates that the observed selectivity originates from differences in the transition state, rather than the ground state. Again, crucial control experiments were performed with the enantiomeric substrate ((−)-CF_3HPNP), which demonstrated a reversal in the hydrolysis kinetics (see Figure 2b).

The effect of pH on the kinetics of the reaction was also investigated. On increasing the pH from 6.5 to 8.0, an increase in catalytic activity (k_{cat}) is observed, but the difference in k_{cat} from using **(+)-1** or **(−)-1** NPs decreases from 38% at pH 6.5 down to 21% at pH 8.0 (Figure 2d). The K_M also shows a general increase going from pH 7.0 to 8.0, due likely to increased competition from the negatively charged form of the buffer used (HEPES or MES) binding at the surface of the NPs. In all cases, at the different pH values no significant differences in K_M were observed for the **(+)-1** and **(−)-1** NPs.

Upon demonstrating with model substrates that enantioselective catalysis is possible with our nanoparticle system, the next goal was to examine ways to increase the enantioselectivity achieved. We reasoned that it was crucial to exploit the multivalency of our system for the formation of additional interactions between the catalyst and the substrate. This would allow precise binding conformations to be formed, giving impetus for enantioselectivity to occur. RNA dinucleotides (3′,5′-NpN, N = U, C, G, A; Figure 3a) emerged as ideal substrates to study,[11] as multiple simultaneous interactions are believed to occur between the metal ions and both the base and phosphate moieties.[12] Aza-crown-Zn^{II} complexes similar to our TACN·Zn^{II} catalysts have been shown to bind specific base moieties, with a special preference for thymine and uracil.[13] The cleavage of these dinucleotides can be followed by HPLC, monitoring the disappearance of the substrates as well as the formation of cyclic ribonucleoside monophosphate (2′,3′-cNMP) and the corresponding nucleoside. The uncatalyzed cleavage of these compounds (UpU, CpC, GpG, and ApA) is extremely slow, ranging from a rate constant of $9.8 \times 10^{-9}\ s^{-1}$ for UpU[6i] (at pH 7) to $1.7 \times 10^{-9}\ s^{-1}$ for ApA.[14]

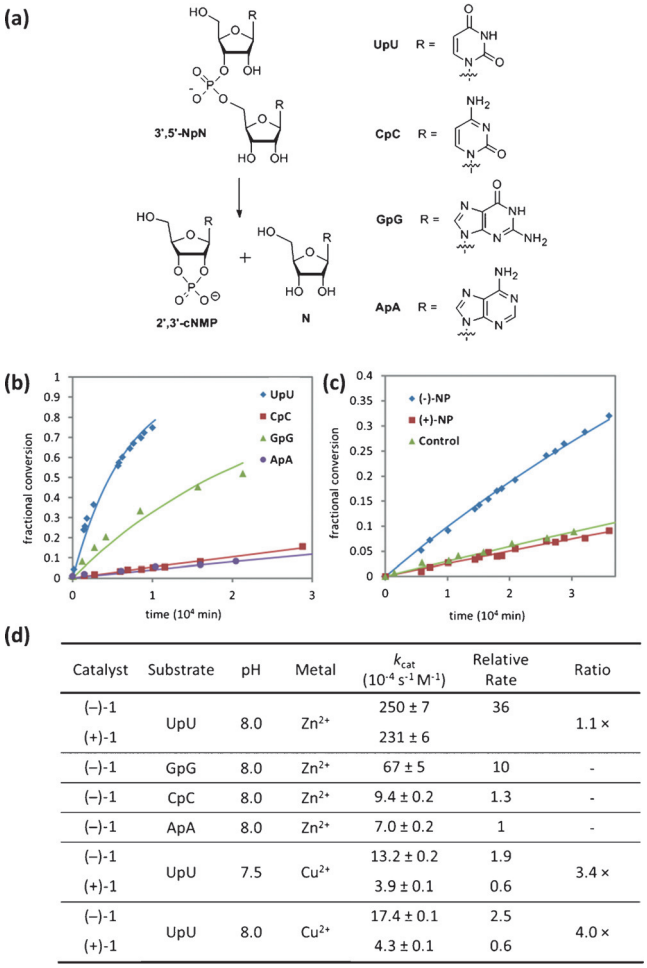

(d)

Catalyst	Substrate	pH	Metal	k_{cat} ($10^{-4}\ s^{-1}\ M^{-1}$)	Relative Rate	Ratio
(−)-1	UpU	8.0	Zn^{2+}	250 ± 7	36	1.1 ×
(+)-1				231 ± 6		
(−)-1	GpG	8.0	Zn^{2+}	67 ± 5	10	-
(−)-1	CpC	8.0	Zn^{2+}	9.4 ± 0.2	1.3	-
(−)-1	ApA	8.0	Zn^{2+}	7.0 ± 0.2	1	-
(−)-1	UpU	7.5	Cu^{2+}	13.2 ± 0.2	1.9	3.4 ×
(+)-1				3.9 ± 0.1	0.6	
(−)-1	UpU	8.0	Cu^{2+}	17.4 ± 0.1	2.5	4.0 ×
(+)-1				4.3 ± 0.1	0.6	

Figure 3. a) Transphosphorylation of dinucleotides. b) Tansphosphorylation of NpN with **(+)-1** NPs, showing fractional conversion over time. c) Cleavage of UpU with **(+)-1** and **(−)-1** NPs in the presence of Cu^{II}; in HEPES pH 8.0, room temperature. d) Summary of rate constants with the different conditions reported. See Supporting Information for further details.

The cleavage of the dinucleotides with **(−)-1** NPs ([TACN·Zn^{II}] = 50 μM) was investigated at pH 8.0. Importantly, the catalysts demonstrated significant substrate specificity in the cleavage of the dinucleotides, promoting the cleavage of UpU with a second-order rate constant of $2.50 \pm 0.07 \times 10^{-2}\ s^{-1}\ M^{-1}$ (Figure 3b). This rate was 3.6 × faster than for GpG ($6.7 \pm 0.5 \times 10^{-3}\ s^{-1}\ M^{-1}$), which in turn reacted 10 × faster than CpC ($9.4 \pm 0.2 \times 10^{-4}\ s^{-1}\ M^{-1}$) and ApA ($7.0 \pm 0.2 \times 10^{-4}\ s^{-1}\ M^{-1}$). The observed selectivity for UpU is in line with the previously reported recognition between related Zn^{II} complexes and uracil (see above).[12] Due to its observed higher activity, further investigations looking at the difference in catalytic activity between **(+)-1** and **(−)-1** NPs were thus performed using UpU as the substrate. Initial trials looking at the difference in catalytic activity between **(+)-1** and **(−)-1** NPs with UpU showed no significant difference when Zn^{II} was employed as the metal ion (Figure 3d). However, a remarkable result was observed when the divalent metal used in the catalysis was switched from Zn^{II}

to Cu^{II}. In this case we observed that at pH 7.5, **(−)-1** NPs ($13.2 \pm 0.2 \times 10^{-4}\ s^{-1}$) were able to catalyze the transphosphorylation of UpU 3.4 × faster than **(+)-1** NPs ($3.9 \pm 0.1 \times 10^{-4}\ s^{-1}\ M^{-1}$; Figure 3d). This difference was further increased at pH 8, with a fourfold difference in rate observed between **(−)-1** NPs ($17.4 \pm 0.1 \times 10^{-4}\ s^{-1}$) and **(+)-1** NPs ($4.3 \pm 0.1 \times 10^{-4}\ s^{-1}\ M^{-1}$; Figure 3c). The rate observed with **(+)-1** NPs is essentially the same as the background rate (control). Thus **(+)-1** NPs are effectively not catalyzing the hydrolysis of UpU at all. These results represent the first example for the enantioselective cleavage of dinucleotides using synthetic metalloenzymes. This has been achieved using the self-assembly of precursors which are by themselves catalytically inactive. The demonstration of enantioselectivity in these biomimetic metallozymes comes one step closer to mimicking the complexity and properties of Nature's own enzymes. By addressing this issue of chirality, we illustrate the opportunities of using self-assembly for the generation of novel chiral synthetic catalysts and the vast potential of this class of nanozymes for further development.

In conclusion, we have shown that chirality is an important design criterion when it comes to assembling nanozymes. While this has so far been overlooked for this class of structures, we show that chiral precursors indeed are able to self-organize on the surface of nanoparticles and form chiral catalytically active pockets. While we are still far away from the performance of an enzyme, we have made a significant step forward by showing for the first time that this class of enzymes is capable of enantiodiscrimination both on model and natural compounds. We show also that the multivalent nature of this system can be expoited to provide enhanced levels of enantioselectivity. This work presents a shift away from the incorporation of an inherently chiral catalyst on the surface of NPs to the self-assembly of chiral catalytic pockets from units that by themselves do not induce enantioselectivity. These systems have the advantages of modularity and greater flexibility in design. As such, this is a major advancement for the development of innovative catalytic systems for enantioselective catalysis.

Acknowledgements

Financial support from the ERC (StG-239898), University of Padova (CPDA138148) and COST (CM1304) is acknowledged.

Keywords: chirality · enzyme mimics · nanozymes · self-assembly · transphosphorylation

[1] a) M. Raynal, P. Ballester, A. Vidal-Ferran, P. W. N. M. van Leeuwen, *Chem. Soc. Rev.* **2014**, *43*, 1734; b) Y. H. Lin, J. S. Ren, X. G. Qu, *Acc. Chem. Res.* **2014**, *47*, 1097; c) H. Wei, E. K. Wang, *Chem. Soc. Rev.* **2013**, *42*, 6060; d) R. Bhandari, R. Coppage, M. R. Knecht, *Catal. Sci. Technol.* **2012**, *2*, 256; e) *Supramolecular Catalysis* (Ed.: P. W. N. M. van Leeuwen), Wiley-VCH, Weinheim, **2008**; f) D. M. Vriezema, M. C. Aragones, J. A. A. W. Elemans, J. J. L. M. Cornelissen, A. E. Rowan, R. J. M. Nolte, *Chem. Rev.* **2005**, *105*, 1445.

[2] a) M. Diez-Castellnou, F. Mancin, P. Scrimin, *J. Am. Chem. Soc.* **2014**, *136*, 1158; b) G. Zaupa, C. Mora, R. Bonomi, L. J. Prins, P. Scrimin, *Chem. Eur. J.* **2011**, *17*, 4879; c) F. Manea, F. B. Houillon, L. Pasquato, P. Scrimin, *Angew. Chem. Int. Ed.* **2004**, *43*, 6165; *Angew. Chem.* **2004**, *116*, 6291.

[3] N. Sträter, W. N. Lipscomb, T. Klabunde, B. Krebs, *Angew. Chem. Int. Ed. Engl.* **1996**, *35*, 2024; *Angew. Chem.* **1996**, *108*, 2158.

[4] a) D. Zaramella, P. Scrimin, L. J. Prins, *J. Am. Chem. Soc.* **2012**, *134*, 8396; b) P. Pengo, S. Polizzi, L. Pasquato, P. Scrimin, *J. Am. Chem. Soc.* **2005**, *127*, 1616.

[5] a) E. Y. Tirel, Z. Bellamy, H. Adams, V. Lebrun, F. Duarte, N. H. Williams, *Angew. Chem. Int. Ed.* **2014**, *53*, 8246; *Angew. Chem.* **2014**, *126*, 8385; b) F. Mancin, P. Scrimin, P. Tecilla, *Chem. Commun.* **2012**, *48*, 5545; c) C. T. Liu, A. A. Neverov, R. S. Brown, *J. Am. Chem. Soc.* **2008**, *130*, 16711; d) C. T. Liu, A. A. Neverov, R. S. Brown, *J. Am. Chem. Soc.* **2008**, *130*, 13870; e) A. A. Neverov, Z. L. Lu, C. I. Maxwell, M. F. Mohamed, C. J. White, J. S. W. Tsang, R. S. Brown, *J. Am. Chem. Soc.* **2006**, *128*, 16398; f) N. H. Williams, B. Takasaki, M. Wall, J. Chin, *Acc. Chem. Res.* **1999**, *32*, 485; g) R. Breslow, J. B. Doherty, G. Guillot, C. Lipsey, *J. Am. Chem. Soc.* **1978**, *100*, 3227; h) N. H. Williams, A. M. Lebuis, J. Chin, *J. Am. Chem. Soc.* **1999**, *121*, 3341.

[6] a) R. Salvio, S. Volpi, R. Cacciapaglia, A. Casnati, L. Mandolini, F. Sansone, *J. Org. Chem.* **2015**, *80*, 5887; b) H. Lönnberg, *Org. Biomol. Chem.* **2011**, *9*, 1687; c) Y. Aiba, J. Sumaoka, M. Komiyama, *Chem. Soc. Rev.* **2011**, *40*, 5657; d) T. Humphry, S. Iyer, O. Iranzo, J. R. Morrow, J. P. Richard, P. Paneth, A. C. Hengge, *J. Am. Chem. Soc.* **2008**, *130*, 17858; e) J. R. Morrow, T. L. Amyes, J. P. Richard, *Acc. Chem. Res.* **2008**, *41*, 539; f) T. Niittymäki, H. Lonnberg, *Org. Biomol. Chem.* **2006**, *4*, 15; g) J. R. Morrow, O. Iranzo, *Curr. Opin. Chem. Biol.* **2004**, *8*, 192; h) P. Molenveld, J. F. J. Engbersen, D. N. Reinhoudt, *Angew. Chem. Int. Ed.* **1999**, *38*, 3189; *Angew. Chem.* **1999**, *111*, 3387; i) W. H. Chapman, R. Breslow, *J. Am. Chem. Soc.* **1995**, *117*, 5462; j) J. Chin, *Curr. Opin. Chem. Biol.* **1997**, *1*, 514.

[7] G. Pieters, L. J. Prins, *New J. Chem.* **2012**, *36*, 1931; a notable example is the hydrolytic kinetic resolution of epoxides by Jacobsen et al. where catalytic activity can be increased by immobilization of catalysts onto NPs: T. Belser, E. N. Jacobsen, *Adv. Synth. Catal.* **2008**, *350*, 967.

[8] P. Rossi, F. Felluga, P. Scrimin, *Tetrahedron Lett.* **1998**, *39*, 7159.

[9] a) F. Manea, C. Bindoli, S. Polizzi, L. Lay, P. Scrimin, *Langmuir* **2008**, *24*, 4120; b) N. R. Jana, X. G. Peng, *J. Am. Chem. Soc.* **2003**, *125*, 14280.

[10] J. P. Horwitz, J. V. Freisler, *J. Med. Chem.* **1970**, *13*, 1024.

[11] a) H. Linjalahti, G. Q. Feng, J. C. Mareque-Rivas, S. Mikkola, N. H. Williams, *J. Am. Chem. Soc.* **2008**, *130*, 4232; b) D. M. Perreault, E. V. Anslyn, *Angew. Chem. Int. Ed. Engl.* **1997**, *36*, 432; *Angew. Chem.* **1997**, *109*, 470; c) M. Oivanen, S. Kuusela, H. Lonnberg, *Chem. Rev.* **1998**, *98*, 961.

[12] a) Q. Wang, H. Lonnberg, *J. Am. Chem. Soc.* **2006**, *128*, 10716; b) Q. Wang, E. Leino, A. Jancso, I. Szilagyi, T. Gajda, E. Hietamaki, H. Lonnberg, *ChemBioChem* **2008**, *9*, 1739.

[13] a) S. Aoki, E. Kimura, *Chem. Rev.* **2004**, *104*, 769; b) M. Shionoya, T. Ikeda, E. Kimura, M. Shiro, *J. Am. Chem. Soc.* **1994**, *116*, 3848.

[14] M. Komiyama, K. Yoshinari, *J. Org. Chem.* **1997**, *62*, 2155.

Received: February 23, 2016
Published online on April 8, 2016